Supplement of Hydrol. Earth Syst. Sci., 27, 3329–3349, 2023
https://doi.org/10.5194/hess-27-3329-2023-supplement

Hydrology and Earth System Sciences
Open Access

Supplement of

An advanced tool integrating failure and sensitivity analysis into novel modeling of the stormwater flood volume

Francesco Fatone et al.

Correspondence to: Bartosz Szeląg (bszelag@tu.kielce.pl)

S1. Uncertainty analysis - GLUE

The problem of parameter identification in the GLUE method is formulated in the form of the Bayesian estimation relation (Beven and Binley, 1992):

$$P(Q/\theta) = \frac{L(Q/\theta)P(\theta)}{\int L(Q/\theta)P(\theta)} \quad (1)$$

where $P(\theta)$ stands for *a priori* (Tab. S1) parameter distribution; the *a priori distribution* of SWMM parameters represents the initial assumption of parameter variability. In the case of mathematical models used to describe surface runoff, usually there is no knowledge of the structure of its distribution and the range of acceptable parameter values resulting from their physical interpretation is known at most. In the analysed case it was assumed that the distribution has uniform character (. In the present discussion the following form of the likelihood function was used (Romanowicz and Beven, 2000):

$$L(Q/\theta) = exp\left(\frac{r_t}{\varepsilon \cdot V(r_t)}\right) \quad (2)$$

V(·) – variance, r_t - mean of the sum of squares of deviations of simulated value from measured value calculated as $r_t = \frac{1}{l} \cdot \sum_{z=1}^{l} \left(Q_o - \widehat{Q}_\iota\right)^2$ (where: Q_o and $\widehat{Q}_\iota$ denote z-th value from the times series of observed and computed flows; ε is a scaling factor for the variance of model residua, used to adjust the width of the confidence intervals. In Kiczko et al. (2018) study, the value of ε was determined, ensuring that 95% of observed discharge points is enclosed by 95% confidence intervals of the model output. Equation (1) is solved using the Monte Carlo method. In the first step, a sample of parameters is developed from an assumed *a priori* distribution. The model (SWMM in this case) is run with each combination of SWMM model parameters (Tab. S1) and from the calculated and measured outflow hydrographs the values of the likelihood function and *a posteriori* distributions are determined.

Table S1. Ranges of SWMM model parameters

Parameters	Unit	Range	
		Min	Max
Coefficient for flow path width (α)	-	2.7	4.7
Retention depth of impervious areas (d_{imp})	mm	0.8	4.8
Retention depth of pervious areas (d_{per})	mm	0.8	6.8
Manning roughness coefficient for impervious areas (n_{imp})	$m^{-1/3} \cdot s$	0.01	0.022
Manning roughness coefficient for pervious areas (n_{per})	$m^{-1/3} \cdot s$	0.16	0.2
Manning roughness coefficient for sewer channels (n_{sew})	$m^{-1/3} \cdot s$	0.01	0.048
Correction coefficient for sub-catchments slope (γ)	-	0.7	1.275
Correction coefficient for percentage of impervious areas (β)	-	0.8	1.375

Table S2. Corrective variants for stormwater system

Variants	Condition
I	0.9·Imp
II	0.9·Imp + (d_{imp} = 3.5mm n_{imp} = 0.035 $m^{-1/3}$·s)
III	0.9·Imp + (d_{imp} = 3.5mm n_{imp} = 0.035 $m^{-1/3}$·s) + (n_{sew} = 0.012 $m^{-1/3}$·s)

S2. Measures of fit between computed results and measurements in a logistic regression model

At the computation stage, the goal was to find such a value of threshold cut off which would provide maximum fit of simulation to measurement data. Thus, the subsequent cut-off values p_m were tested until the best fit of measurement data and computation results was obtained (SENS, SPEC → max of value). The fit of the calculation results to measurements was evaluated with the following measures: sensitivity (SENS – determines correctness of classification in a set when the threshold values are exceeded), specificity (SPEC – determines correctness of classification in a set when the threshold values are not exceeded) and accuracy (Acc), which were discussed in detail in Harrell (2001).

- accuracy (Acc)

$$Acc = \frac{TP+TN}{TP+TN+FP+F} \tag{3}$$

- sensitivity (SENS)

$$Sens = \frac{TP}{TP+FN} \tag{4}$$

and specificity (SPEC)

$$Spec = \frac{TN}{TN+FP} \tag{5}$$

where $TP, TN, FP,$ and FN denote true positives (correctly identified of the $\kappa \geq 13$ $m^3 \cdot ha^{-1}$), true negatives (correctly identified lack of $\kappa \geq 13$ $m^3 \cdot ha^{-1}$), false positives ($\kappa < 13$ $m^3 \cdot ha^{-1}$ incorrectly identified as $\kappa \geq 13$ $m^3 \cdot ha^{-1}$) and false negatives ($\kappa \geq 13$ $m^3 \cdot ha^{-1}$ incorrectly identified as $\kappa < 13$ $m^3 \cdot ha^{-1}$), respectively.

S3. Verification LRM model using SWMM

The calculations included the following steps:

a) selection of two input data (x1, x2) to change; the values of the other parameters were taken as the mean of the data according to Table 1,

b) determination of combinations x1, x2 for verification calculations such that: 1.2·x1 - 1.2·x1, 1.2·x1 - x2, 1.2·x1 - 0.8·x2; x1 - 1.2·x2, x1 - x2, x1 - 0.8·x2; 0.8·x2 - 1.2·x1, 0.8·x2 - x1, 0.8·x2 - 0.8·x1; all combinations of catchment and sewer network characteristics were analysed in this study, resulting in a total of 135 verification variants for 3 sub-catchments (135·35·3 = 14175 simulations),

c) modification of sub-catchment characteristics according to point b)

d) calculation with a logit model and SWMM of the value of the specific flood volume.

S4. Regional model of convective rainfall

To calculate the convective rainfall, the regional rainfall model for Poland was used (Kupczyk and Suligowski, 2000; Suligowski, 2004). In this model the rainfall depth for the assumed rainfall duration is determined from the formula:

$$\mathrm{P_{con}}(\mathrm{t_r}) = \mathrm{a_1} \cdot \mathrm{t_r^2} + \mathrm{a_2} \cdot \mathrm{t_r} + \mathrm{a_0} \tag{6}$$

where: t_r – duration of rainfall (min); $P_{con}(t_r)$ – maximum convective rainfall depth (mm); a_0, a_1, a_2 – empirical coefficients determined by the method of least squares. The model includes data for 30 rainfall stations in Poland, for which a_i (a_0, a_1, a_2) coefficients were determined using rainfall data from the period of 20 - 30 years (Suligowski 2004). For the catchment area covered by the calculations (świętokrzyskie voivodship) the values are as follows: $a_0 = 6.55$; $a_1 = -1.10$, $a_2 = 6.68$.

S5. Probability of stormwater network failure

The probability of specific flood volume for the limiting value of $p_{m,cr}$ (exceeding it indicates that $\kappa > 13$ $m^3 \cdot ha^{-1}$ can be written as:

$$p_{m,cr} = \frac{exp(\boldsymbol{X})}{1+exp(\boldsymbol{X})} \tag{7}$$

By transforming equation (7), it can be stated that:

$$\boldsymbol{X} = ln\left(\frac{p_{m,cr}}{1-p_{m,cr}}\right) \tag{8}$$

Knowing that X is a linear combination of the independent variables, the relationship can be written:

$$\boldsymbol{X} = \boldsymbol{X}_{rain} + \boldsymbol{X}_{catchm} + \left(\sum_{k=1}^{m} \alpha_k \cdot x_k + \alpha_{nsew} \cdot n_{sew}\right) \tag{9}$$

Comparing sides (8), (9) obtained:

$$\boldsymbol{X}_{rain} + \boldsymbol{X}_{catchm} + \left(\sum_{k=1}^{m} \alpha_k \cdot x_k + \alpha_{nsew} \cdot n_{sew}\right) = ln\left(\frac{p_{m,cr}}{1-p_{m,cr}}\right) \tag{10}$$

By transforming equation (10), the value of n_{sew} can be determined from the formula:

$$n_{sew} = \frac{1}{\alpha_{nsew}} \cdot \left[ln\left(\frac{p_{m,cr}}{1-p_{m,cr}}\right) - \boldsymbol{X}_{rain} - \boldsymbol{X}_{catch} \quad - \sum_{k=1}^{m} \alpha_k \cdot x_k\right] \tag{11}$$

Table. S3. Values of coefficients (α_i), standard deviations (σ_i), test probabilities (p) for the logit model to calculate the probability of specific flood volume.

Variable	Value (α_i)	St. derivation (σ_i)	p – test
Intercept	-54.146	1.863	< 0.0001
t_r	-0.218	0.001	< 0.0001
P_t	4.055	0.036	< 0.0001
α	0.235	0.012	< 0.0001
n_{imp}	-79.397	1.251	< 0.0001
d_{imp}	-0.072	0.006	< 0.0001
β	6.233	0.051	< 0.0001
γ	0.333	0.043	< 0.0001
n_{sew}	234.125	1.145	< 0.0001
Imp	79.403	4.836	< 0.0001
Vk	-0.010	0.000	< 0.0001
Gk	-1967.036	113.936	< 0.0001
Jkp	-20.331	6.775	0.0027
Impd	42.912	2.389	< 0.0001
Gkd	-1169.004	66.862	< 0.0001

Table. S4. Agreement of the results of calculating the probability of exceeding the specific flood volume with the logistic regression model (LRM) and SWMM

	Sub - catchment								
t_r [min]	J	K	L	M	N	O	P	R	S
variant I									
30	+	+	+	+	+	+	+	+	+
40	+	+	+	+	+	+	+	+	+
50	+	+	+	+	+	+	+	+	+
60	+	+	+	+	+	+	+	-	-
variant III									
30	+	+	+	+	+	+	+	+	+
40	+	+	+	+	+	+	+	+	+
50	+	+	+	+	+	+	+	+	+
60	+	+	+	+	+	+	-	-	+

Table S5. Computational scenarios assumed for the verification of the obtained LRM by means of SWMM

Var		Impd			Gk			Gkd			Vk			Jkp		
	±	+20	0	-20	+20	0	-20	+20	0	-20	+20	0	-20	+20	0	-20
	+20	+	+	+	+	+	+	+	+	+	+	+	+	+	+	+
	0	+	+	+	+	+	+	+	+	+	+	+	+	+	+	+
Imp	-20	+	+	+	+	+	+	+	+	+	+	+	+	+	+	+
	+20				+	+	+	+	+	+	+	+	+	+	+	+
	0				+	+	+	+	+	+	+	+	+	+	+	+
Impd	-20				+	+	+	+	+	+	+	+	+	+	+	+
	+20							+	+	+	+	+	+	+	+	+
	0							+	+	+	+	+	+	+	+	+
Gk	-20							+	+	+	+	+	+	+	+	+
	+20										+	+	+	+	+	+
	0										+	+	+	+	+	+
Gkd	-20										+	+	+	+	+	+
	+20													+	+	+
	0													+	+	+
Vk	-20													+	+	+

Table S6. Results of simulating the number of events (κ > 13 $m^3 \cdot ha^{-1}$) by the LRM for sub - catchment J

Var		Impd			Gk			Gkd			Vk			Jkp		
	±	+20	0	-20	+20	0	-20	+20	0	-20	+20	0	-20	+20	0	-20
	+20	17	14	14	14	14	16	14	14	15	14	14	14	14	14	14
	0	14	12	7	7	12	14	10	12	14	12	12	14	12	12	12
Imp	-20	7	7	4	5	7	8	5	7	7	6	7	7	7	7	7
	+20				13	14	14	14	14	14	14	14	14	14	14	14
	0				7	12	14	10	12	14	12	12	13	12	12	12
Impd	-20				6	7	12	7	7	10	7	7	8	7	7	7
	+20							7	14	10	7	14	8	7	14	7
	0							10	12	14	12	12	13	12	12	12
Gk	-20							14	7	14	14	7	14	14	7	14
	+20										9	14	7	10	14	10
	0										12	12	8	12	12	12
Gkd	-20										14	7	14	14	7	14
	+20													12	14	12
	0													12	12	12
Vk	-20													13	7	13

Table S7. Differences in simulation results of the number of events (κ > 13 $m^3 \cdot ha^{-1}$) by LRM and SWMM for sub-catchment J

Var		Impd			Gk			Gkd			Vk			Jkp		
	±	+20	0	-20	+20	0	-20	+20	0	-20	+20	0	-20	+20	0	-20
	+20	3	3	2	2	3	2	2	3	3	2	3	3	2	3	2
	0	3	2	1	2	2	2	2	2	2	3	2	3	2	2	2
Imp	-20	1	1	0	1	1	1	1	1	0	1	1	1	1	1	1
	+20				2	3	2	2	3	3	2	3	2	2	3	2
	0				2	2	2	2	2	2	3	2	3	2	2	2
Impd	-20				1	1	3	1	1	2	1	1	2	1	1	1
	+20							1	3	2	1	3	2	2	3	1
	0							2	2	2	3	2	3	2	2	2
Gk	-20							3	1	2	3	1	3	2	1	2
	+20										2	3	2	2	3	2
	0										2	2	3	2	2	2
Gkd	-20										2	1	2	2	1	3
	+20													2	3	2
	0													2	2	2
Vk	-20													2	1	2

Table S8. Results of simulating the number of events (κ > 13 $m^3 \cdot ha^{-1}$) by the LRM model for sub-catchment O

Var		Impd			Gk			Gkd			Vk			Jkp		
	±	+20	0	-20	+20	0	-20	+20	0	-20	+20	0	-20	+20	0	-20
	+20	14	14	8	9	14	14	13	14	14	12	14	14	14	14	12
	0	14	7	5	6	7	12	7	7	8	7	7	9	7	7	7
Imp	-20	7	5	3	4	5	7	4	5	5	4	5	6	5	5	4
	+20				8	14	14	12	14	14	11	14	14	13	14	13
	0				6	7	12	7	7	8	7	7	9	7	7	7
Impd	-20				4	5	7	5	5	6	4	5	7	5	5	5
	+20							5	14	7	5	14	7	6	14	6
	0							7	7	8	7	7	9	7	7	7
Gk	-20							11	5	13	8	5	14	12	5	12
	+20										6	14	8	7	14	7
	0										7	7	9	7	7	7
Gkd	-20										7	5	12	8	5	8
	+20													7	14	7
	0													7	7	7
Vk	-20													9	5	10

Table S9. Differences in simulation results of the number of events (κ > 13 $m^3 \cdot ha^{-1}$) by LRM and SWMM for sub – catchment O

Var		Impd			Gk			Gkd			Vk			Jkp		
	±	+20	0	-20	+20	0	-20	+20	0	-20	+20	0	-20	+20	0	-20
	+20	3	2	1	2	2	3	2	2	2	2	2	3	3	2	2
	0	2	2	1	1	2	3	1	2	2	1	2	2	2	2	1
Imp	-20	1	1	0	0	1	1	1	1	1	1	1	2	0	1	1
	+20				1	2	3	3	2	1	2	2	2	3	2	3
	0				1	2	3	1	2	2	1	2	2	2	2	1
Impd	-20				1	1	0	1	1	1	1	1	1	1	1	1
	+20							1	2	1	1	2	2	1	2	1
	0							1	2	2	1	2	2	2	2	1
Gk	-20							2	1	2	2	1	3	2	1	3
	+20										1	2	2	1	2	1
	0										1	2	2	2	2	1
Gkd	-20										1	1	3	1	1	1
	+20													1	2	1
	0													2	2	1
Vk	-20													2	1	3

Table S10. Results of simulating the number of events (κ > 13 $m^3 \cdot ha^{-1}$) by the LRM for sub-catchment S

Var		Impd			Gk			Gkd			Vk			Jkp		
	±	+20	0	-20	+20	0	-20	+20	0	-20	+20	0	-20	+20	0	-20
	+20	22	16	14	14	16	21	14	16	16	14	16	21	16	16	16
	0	15	14	9	11	14	14	14	14	14	12	14	14	14	14	14
Imp	-20	13	7	5	5	7	12	5	7	7	6	7	11	7	7	7
	+20				14	16	21	14	16	15	14	16	19	15	16	15
	0				11	14	14	14	14	14	12	14	14	14	14	14
Impd	-20				7	7	14	8	7	9	7	7	13	9	7	9
	+20							10	16	12	7	16	14	11	16	11
	0							14	14	14	12	14	14	14	14	14
Gk	-20							14	7	14	14	7	16	14	7	14
	+20											16	14	14	16	14
	0											14	14	14	14	14
Gkd	-20											7	14	14	7	14
	+20														16	12
	0														14	14
Vk	-20														7	14

Table S11. Differences in simulation results of the number of events (κ > 13 $m^3 \cdot ha^{-1}$) by LRM and SWMM for sub – catchment S

Var		Impd			Gk			Gkd			Vk			Jkp		
	±	+20	0	-20	+20	0	-20	+20	0	-20	+20	0	-20	+20	0	-20
	+20	4	3	3	2	3	2	3	3	2	3	3	4	3	3	2
	0	3	3	2	2	2	2	2	2	2	2	2	2	3	2	2
Imp	-20	3	1	1	1	1	2	1	1	1	0	1	2	1	1	1
	+20				2	3	4	3	3	2	2	3	3	3	3	2
	0				2	2	2	2	2	2	2	2	2	3	2	2
Impd	-20				2	1	3	1	1	1	0	1	3	2	1	1
	+20							2	3	2	1	3	3	2	3	2
	0							2	2	2	2	2	2	3	2	2
Gk	-20							2	1	3	2	1	3	2	1	2
	+20											3	3	2	3	2
	0											2	2	3	2	2
Gkd	-20											1	3	2	1	2
	+20														3	2
	0														2	2
Vk	-20														1	2

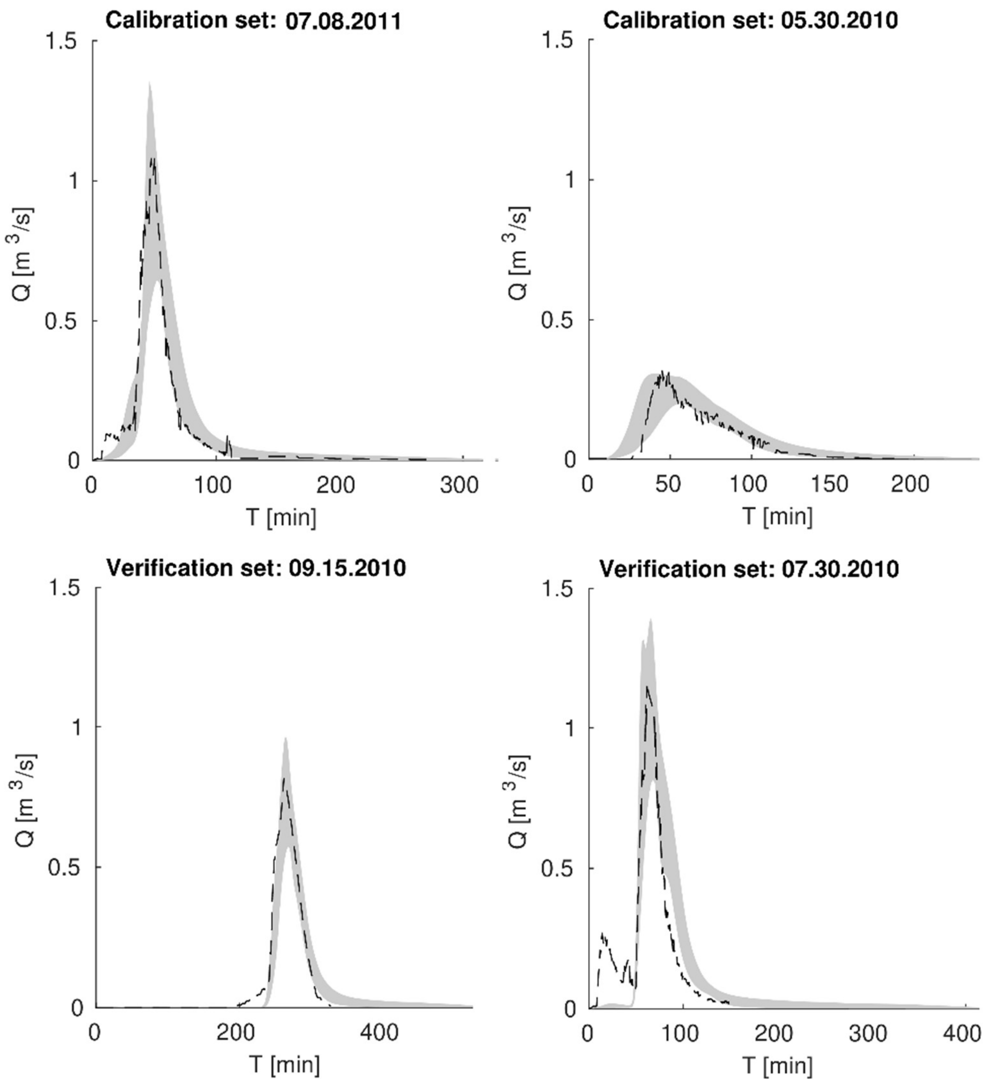

Figure S1. Comparison of the measured hydrographs of stormwater runoff from the catchment with 95% confidence intervals determined via the SWMM model.

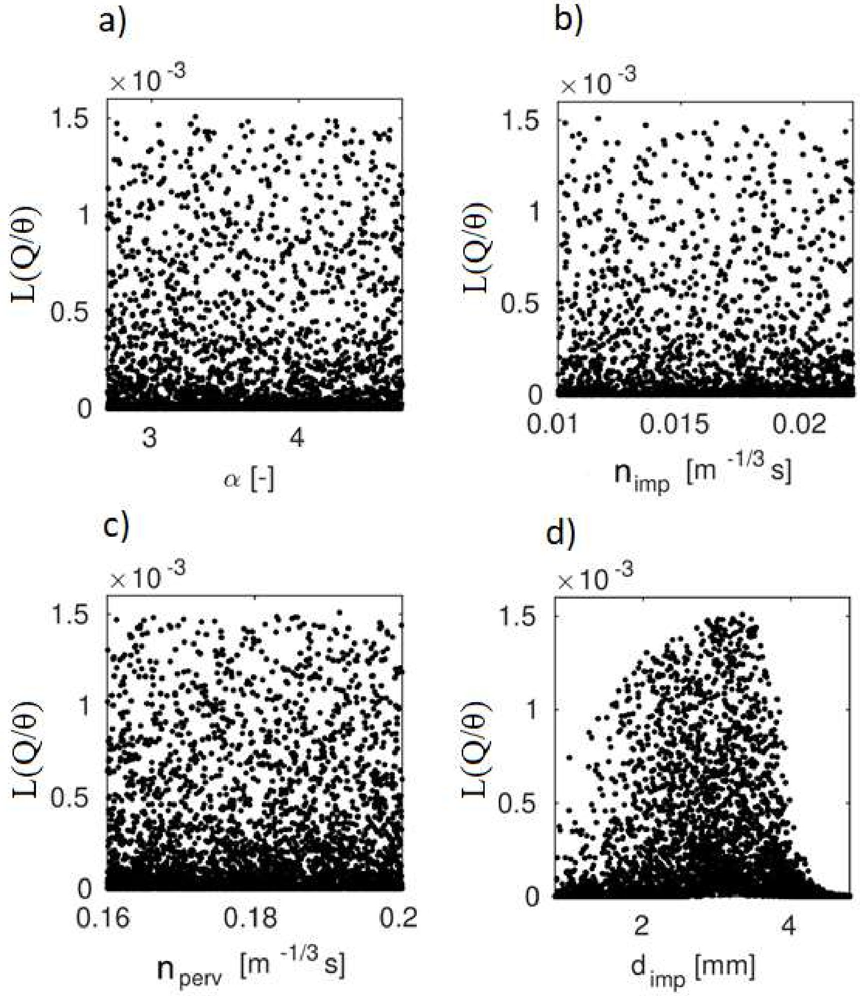

Figure S2. Influence of (a) coefficient for flow path width (α), (b) Manning roughness coefficient for impervious areas (n_{imp}), (c) Manning roughness coefficient for pervious areas (n_{per}) and retention depth of impervious areas (d_{imp}) on the likelihood function (L(Q/θ)).

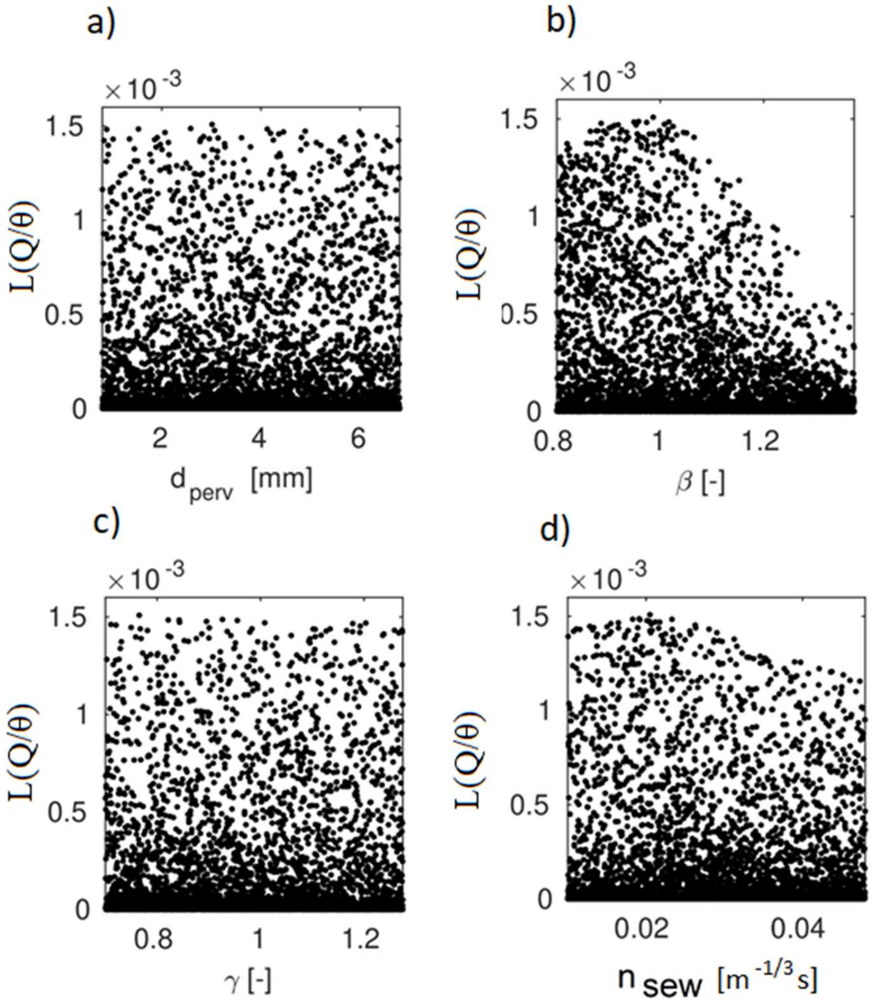

Figure S3. Influence of (a) retention depth of pervious areas (d_{perv}), (b) correction coefficient for percentage of impervious areas (β), (c) correction coefficient for sub-catchments slope (γ) and Manning roughness coefficient for sewer channels (n_{sew}) on the likelihood function (L(Q/θ)).

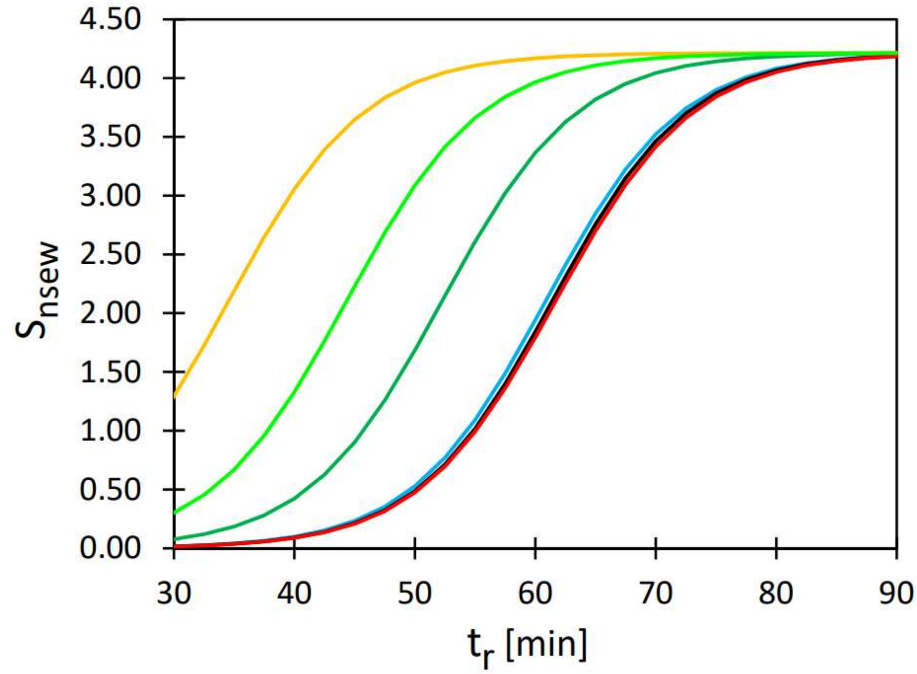

Figure S4. Influence of rainfall duration (t_r) depending on catchment and stormwater network characteristics (Imp, Impd, Vk, Jkp, Gk) on the sensitivity coefficient S_{nsew}.

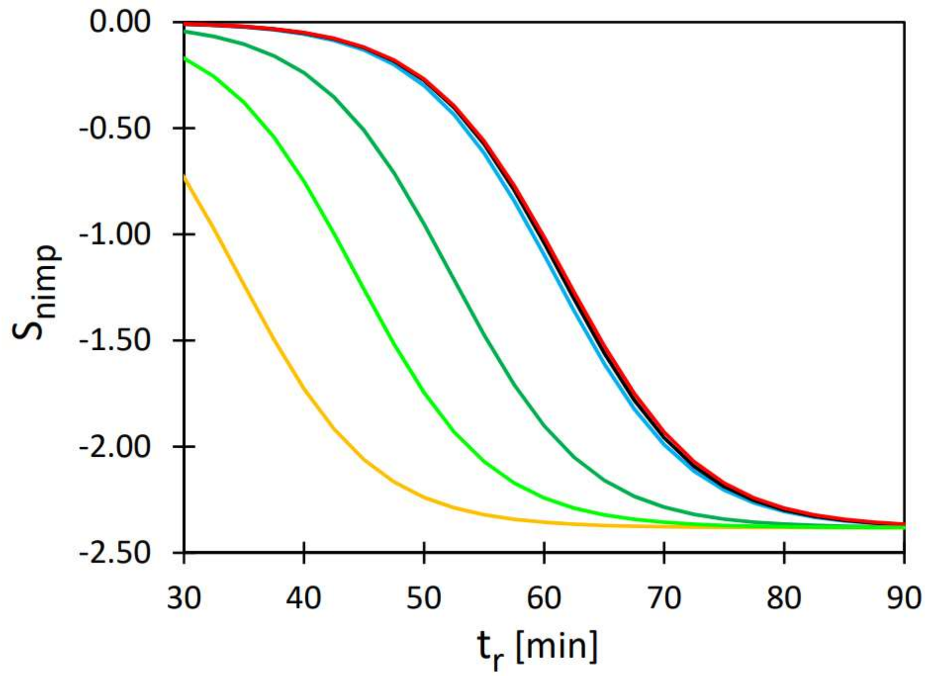

Figure S5. Influence of rainfall duration (t_r) depending on catchment and stormwater network characteristics (Imp, Impd, Vk, Jkp, Gk) on the sensitivity coefficient S_{nimp}.

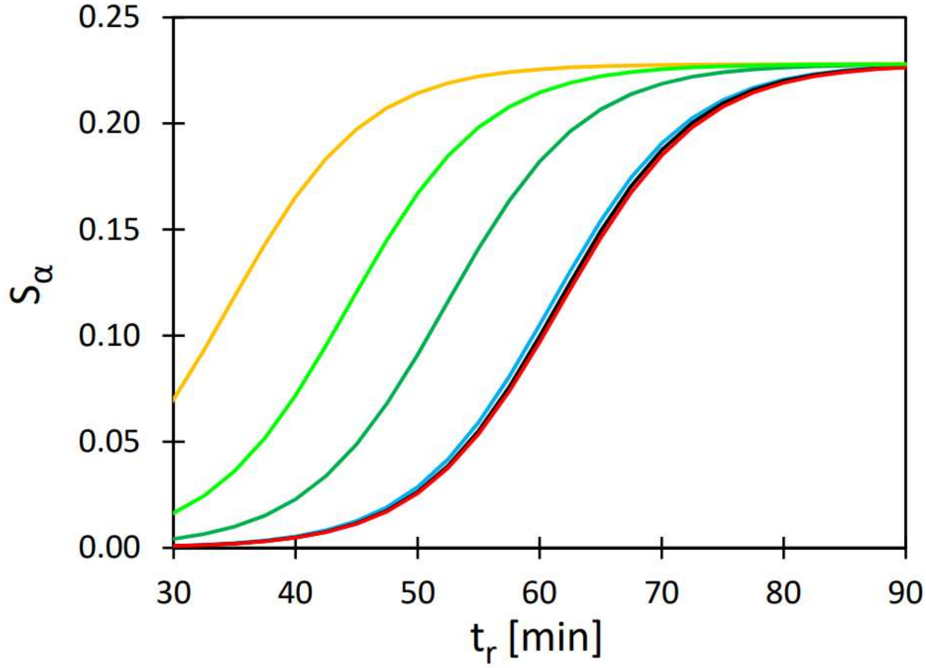

Figure S6. Influence of rainfall duration (t_r) depending on catchment and stormwater network characteristics (Imp, Impd, Vk, Jkp, Gk) on the sensitivity coefficient S_{α}.

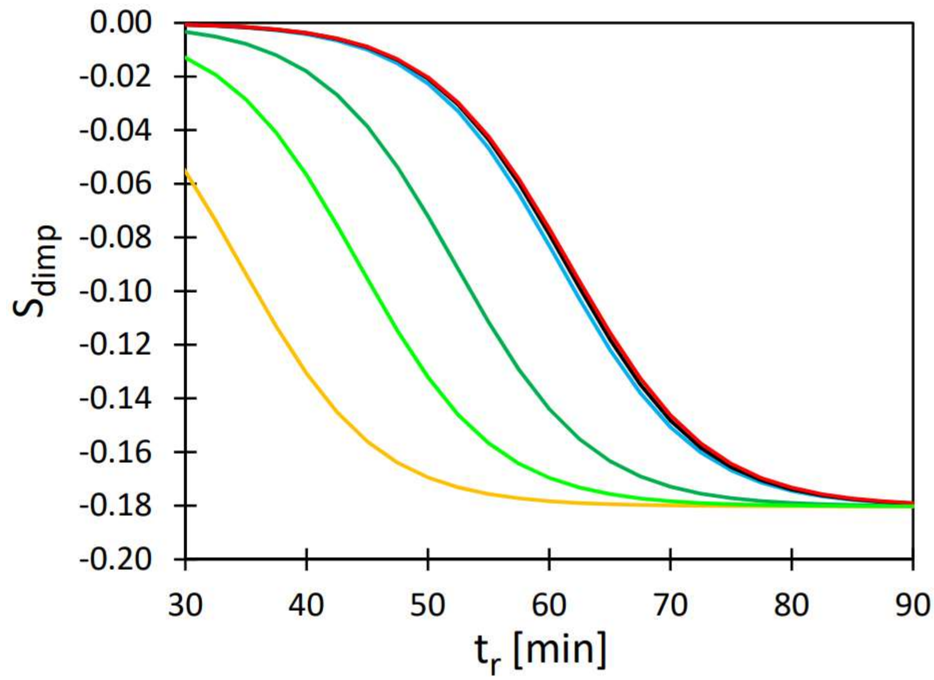

Figure S7. Influence of rainfall duration (t_r) depending on catchment and stormwater network characteristics (Imp, Impd, Vk, Jkp, Gk) on the sensitivity coefficient S_{dimp}.

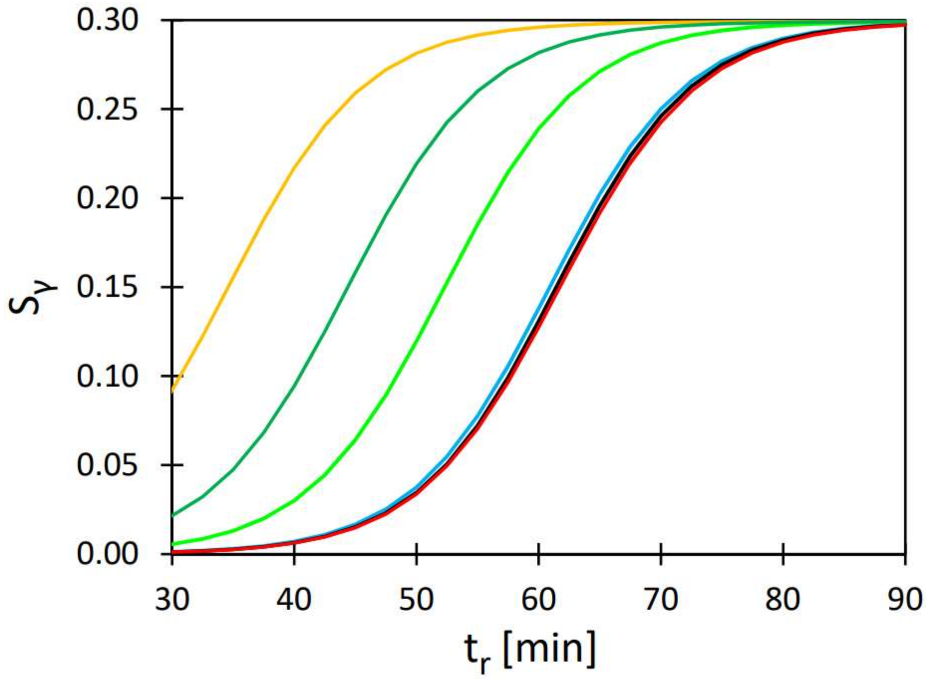

Figure S8. Influence of rainfall duration (t_r) depending on catchment and stormwater network characteristics (Imp, Impd, Vk, Jkp, Gk) on the sensitivity coefficient S_γ.

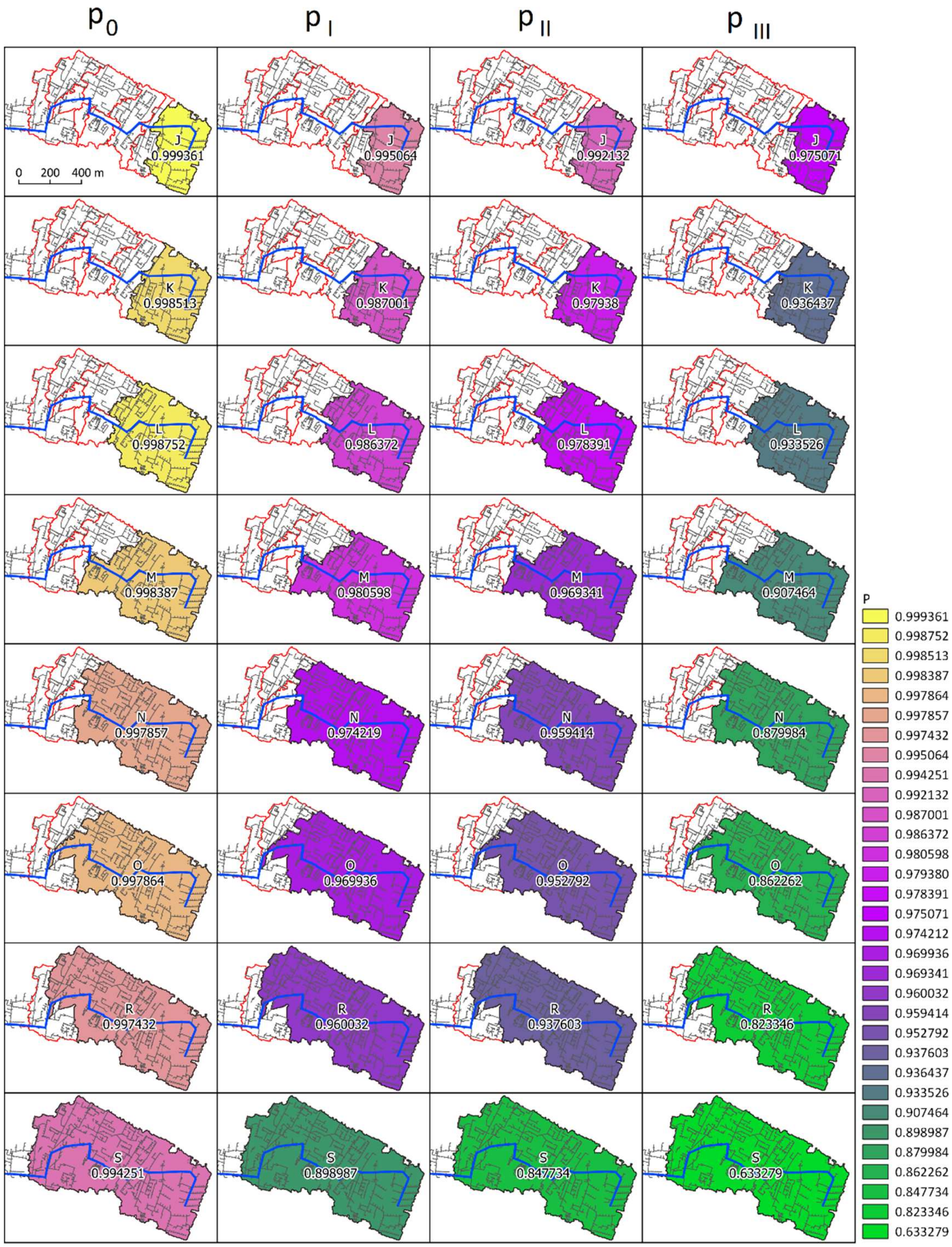

Figure S9. Probability of specific flood volume for separate sub-catchments (J, K, L, M, N, O, R, S) for the current state and corrective variants (I, II, III).

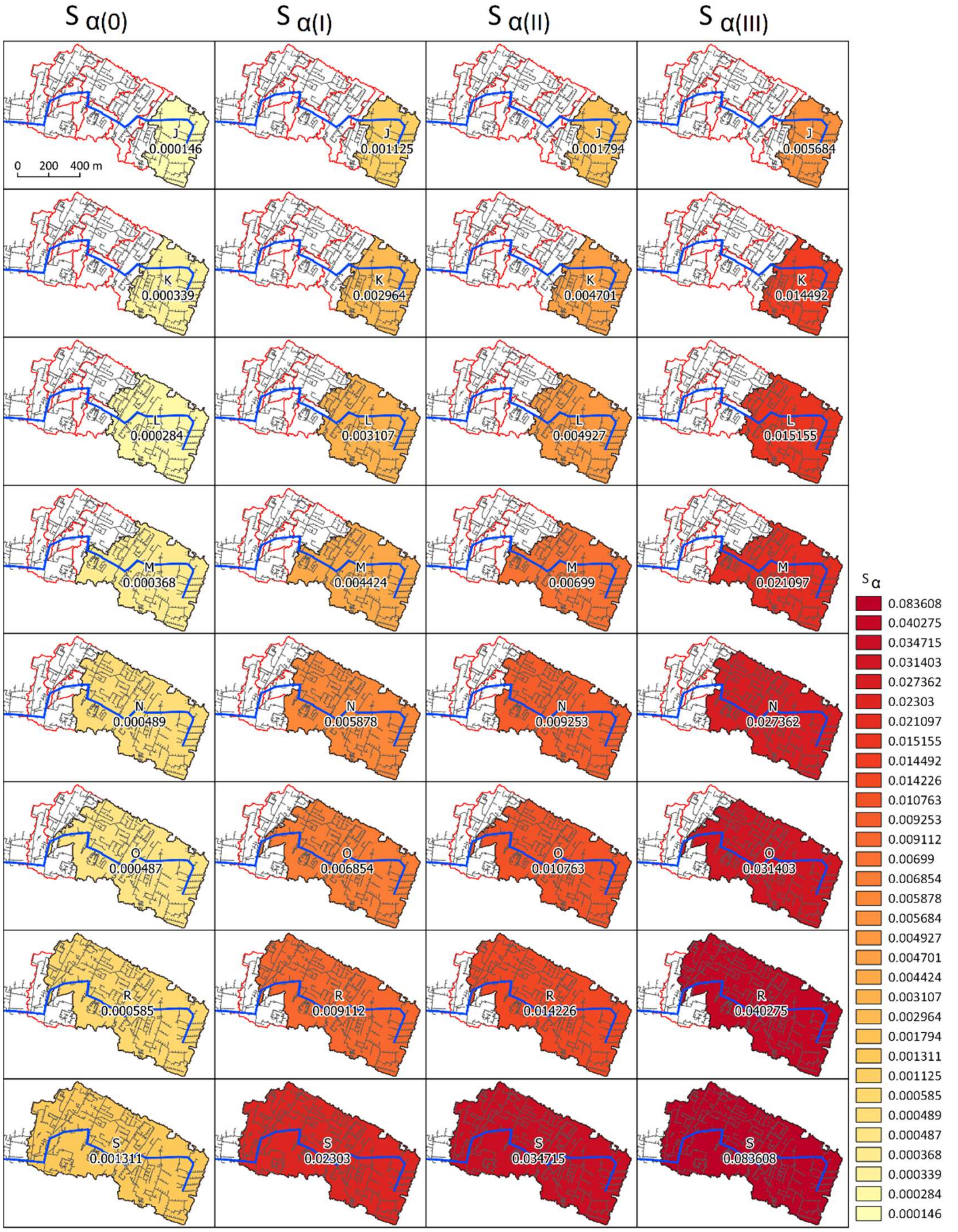

Figure S10. Sensitivity coefficient S_α for separated of the sub-catchments (J, K, L, M, N, O, R, S) for the current state and corrective variants (I, II, III).

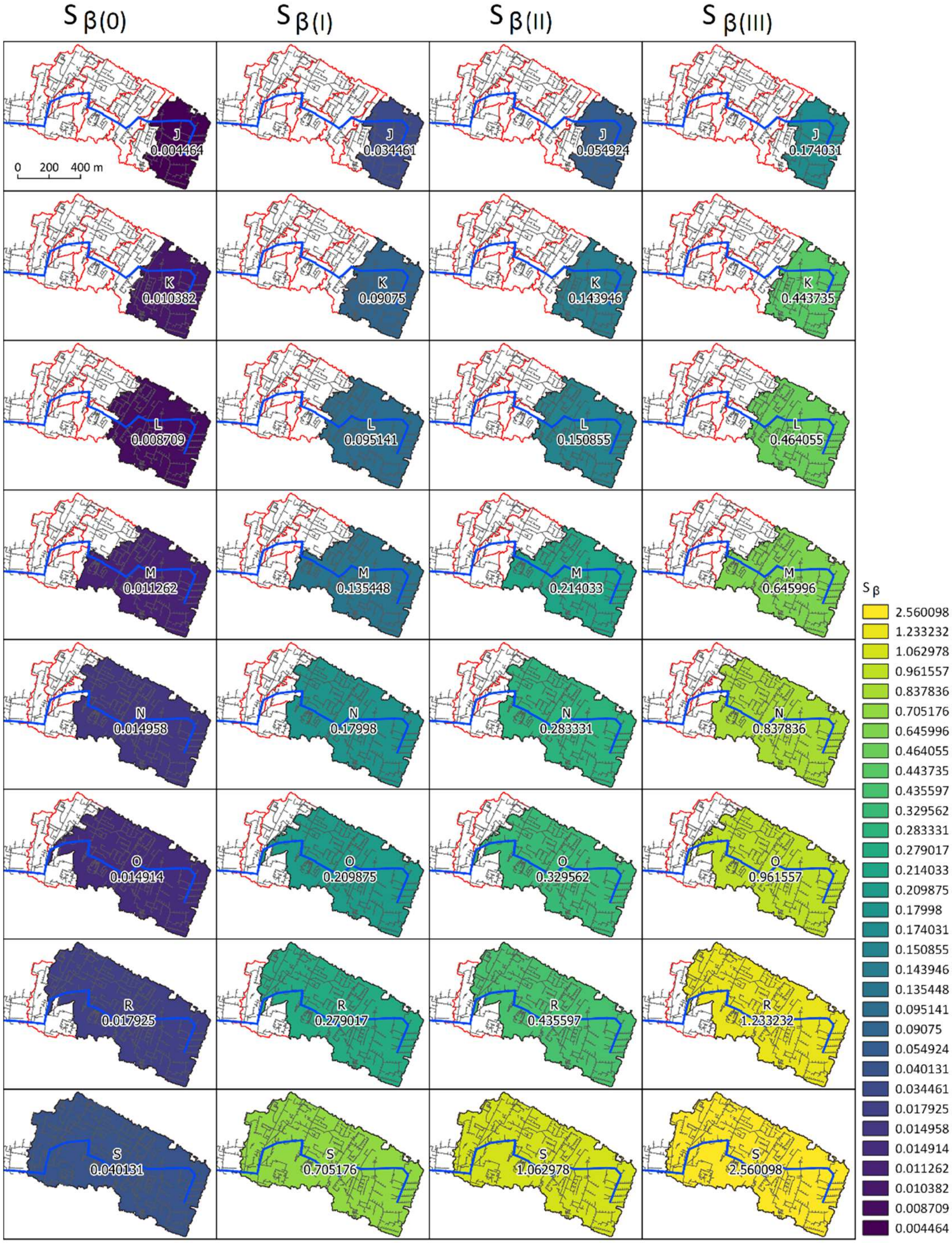

Figure S11. Sensitivity coefficient S_{β} for separated of the sub-catchments (J, K, L, M, N, O, R, S) for the current state and corrective variants (I, II, III).

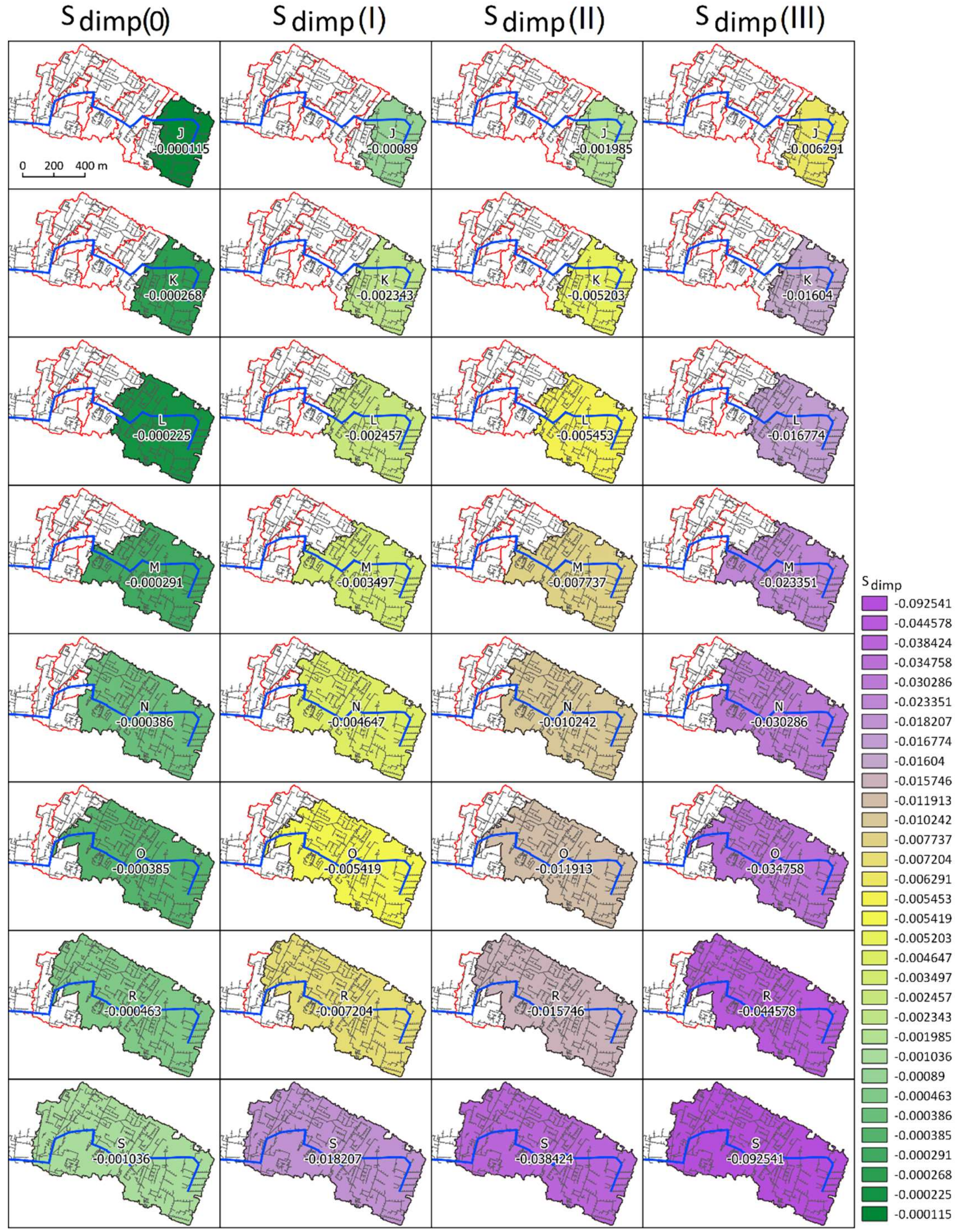

Figure S12. Sensitivity coefficient S_{dimp} for separated of the sub-catchments (J, K, L, M, N, O, R, S) for the current state and corrective variants (I, II, III).

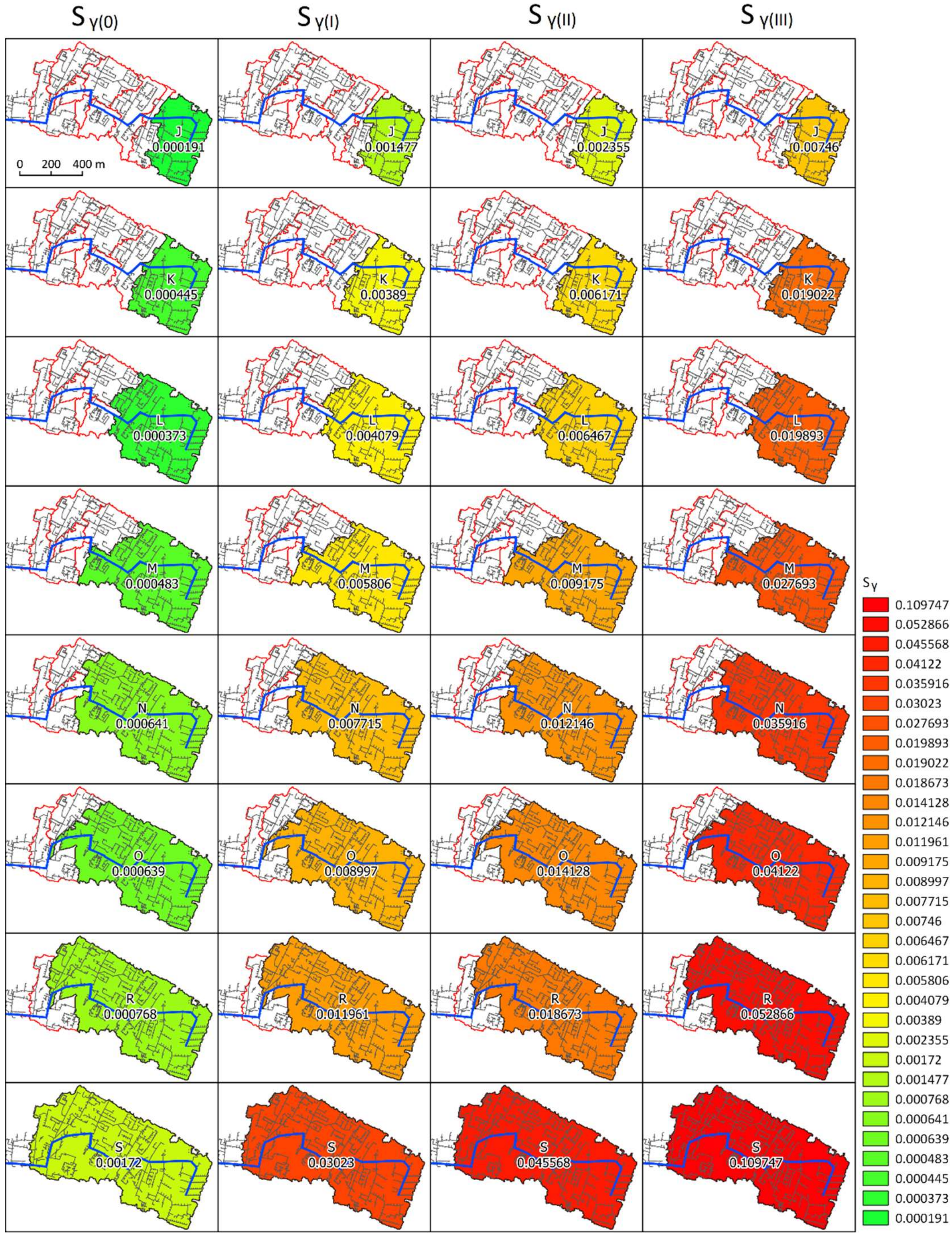

Figure S13. Sensitivity coefficient S_γ for separated of the sub-catchments (J, K, L, M, N, O, R, S) for the current state and corrective variants (I, II, III).

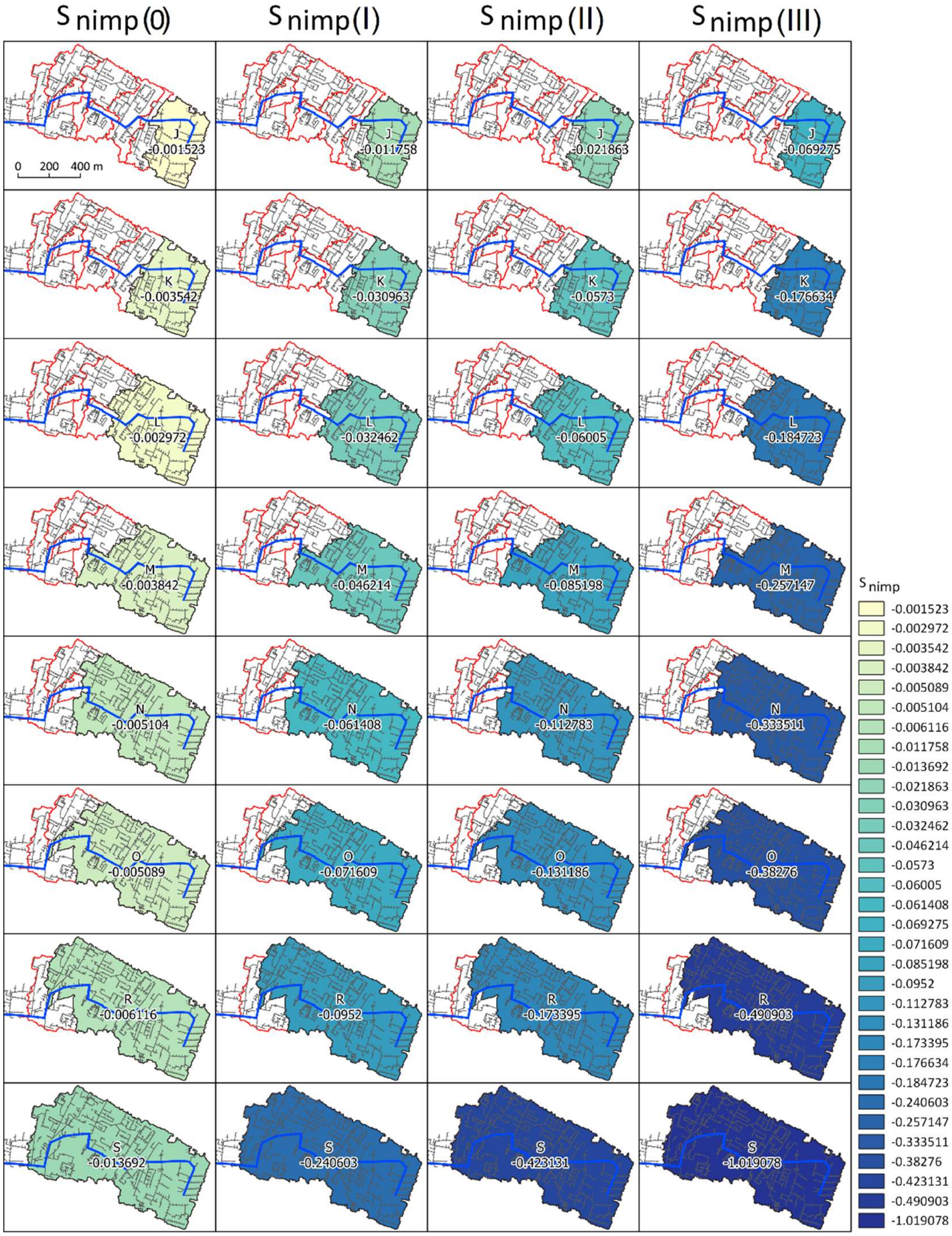

Figure S14. Sensitivity coefficient S_{nimp} for separated of the sub-catchments (J, K, L, M, N, O, R, S) for the current state and corrective variants (I, II, III).

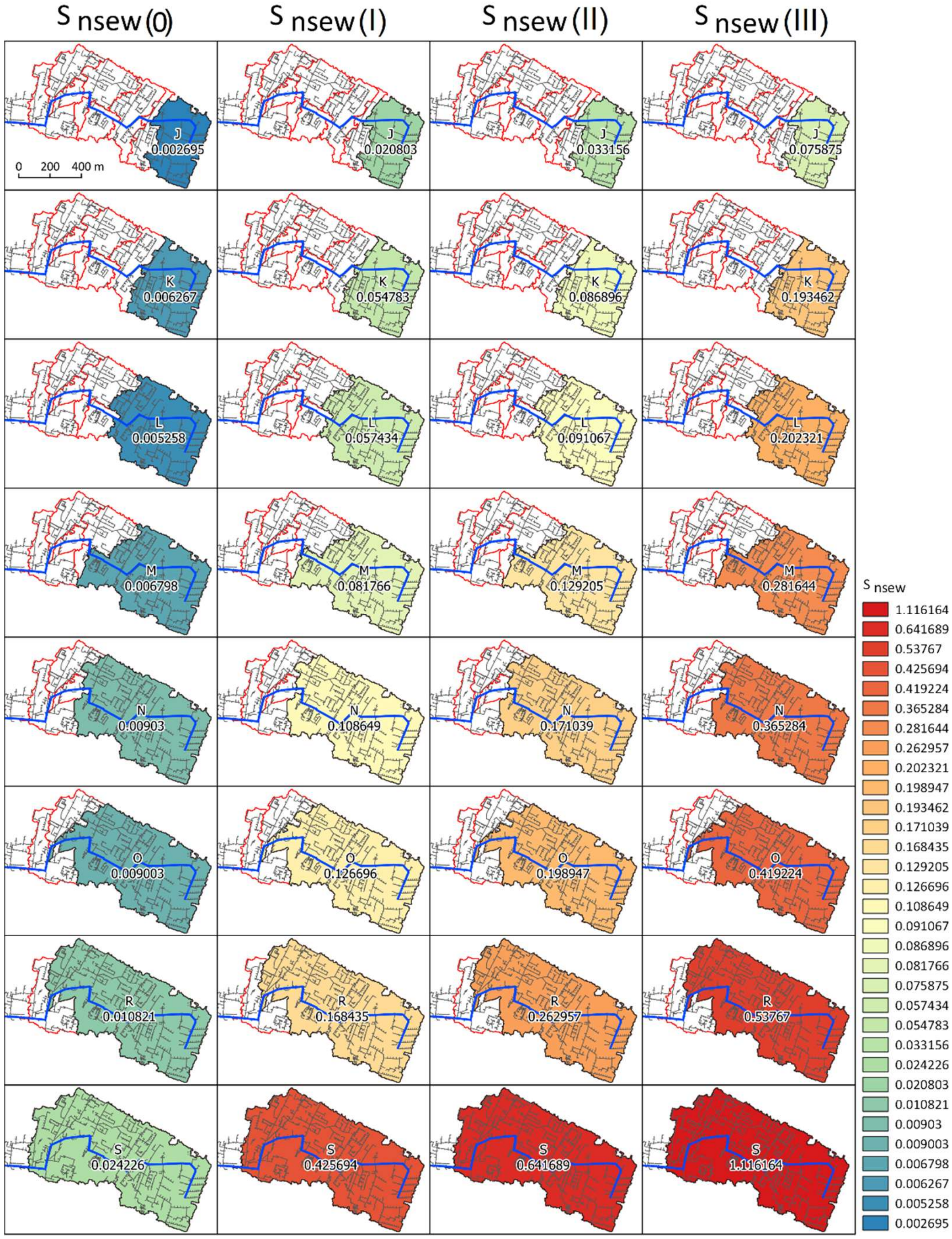

Figure S15. Sensitivity coefficient S_{nsew} for separated of the sub-catchments (J, K, L, M, N, O, R, S) for the current state and corrective variants (I, II, III).

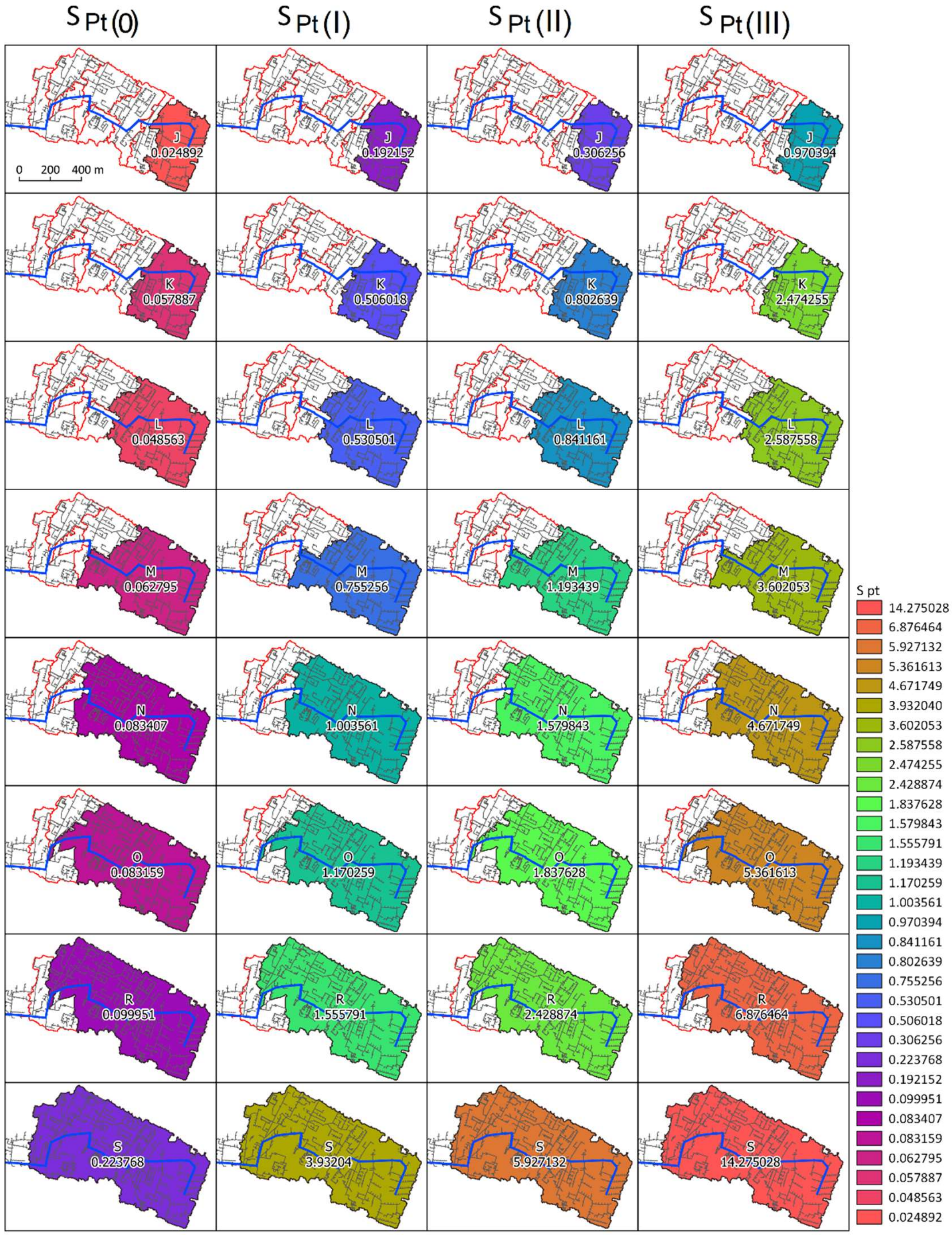

Figure S16. Sensitivity coefficient S_{Pt} for separated of the sub-catchments (J, K, L, M, N, O, R, S) for the current state and corrective variants (I, II, III).

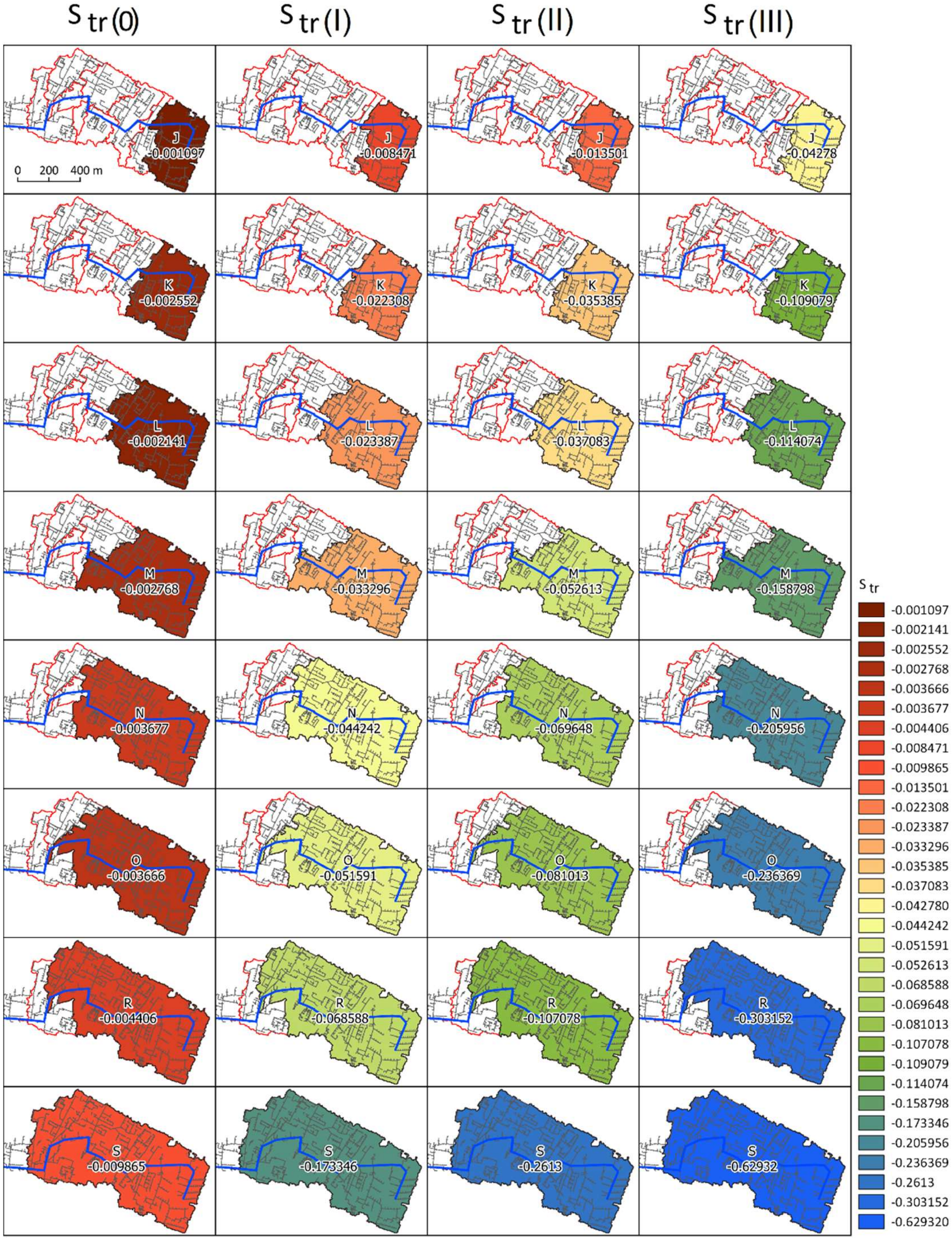

Figure S17. Sensitivity coefficient S_{tr} for separated of the sub-catchments (J, K, L, M, N, O, R, S) for the current state and corrective variants (I, II, III).

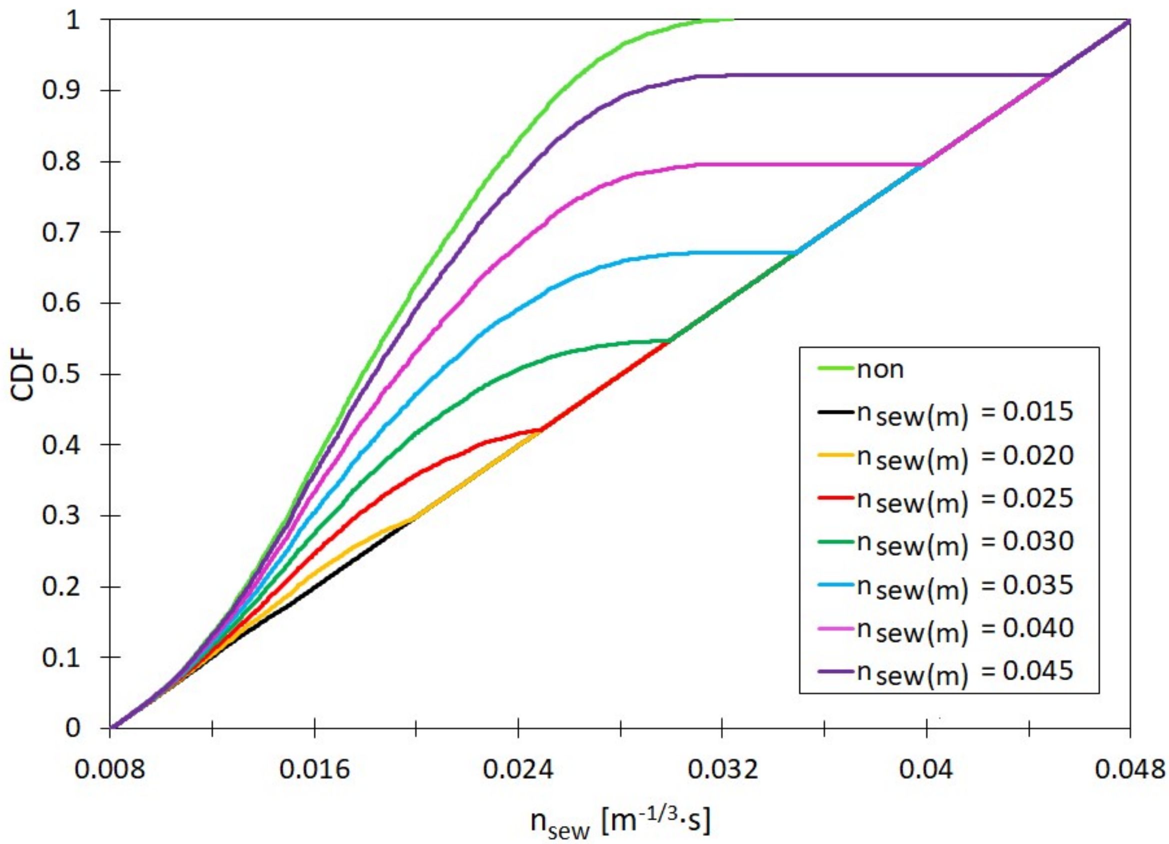

Figure S18. Empirical distributions of Manning roughness coefficients of channels (n_{sew}) for $n_{sew(m)}$=0.015 – 0.045 $m^{-1/3}\cdot s$, Imp = 0.35 and Impd = 0.42.

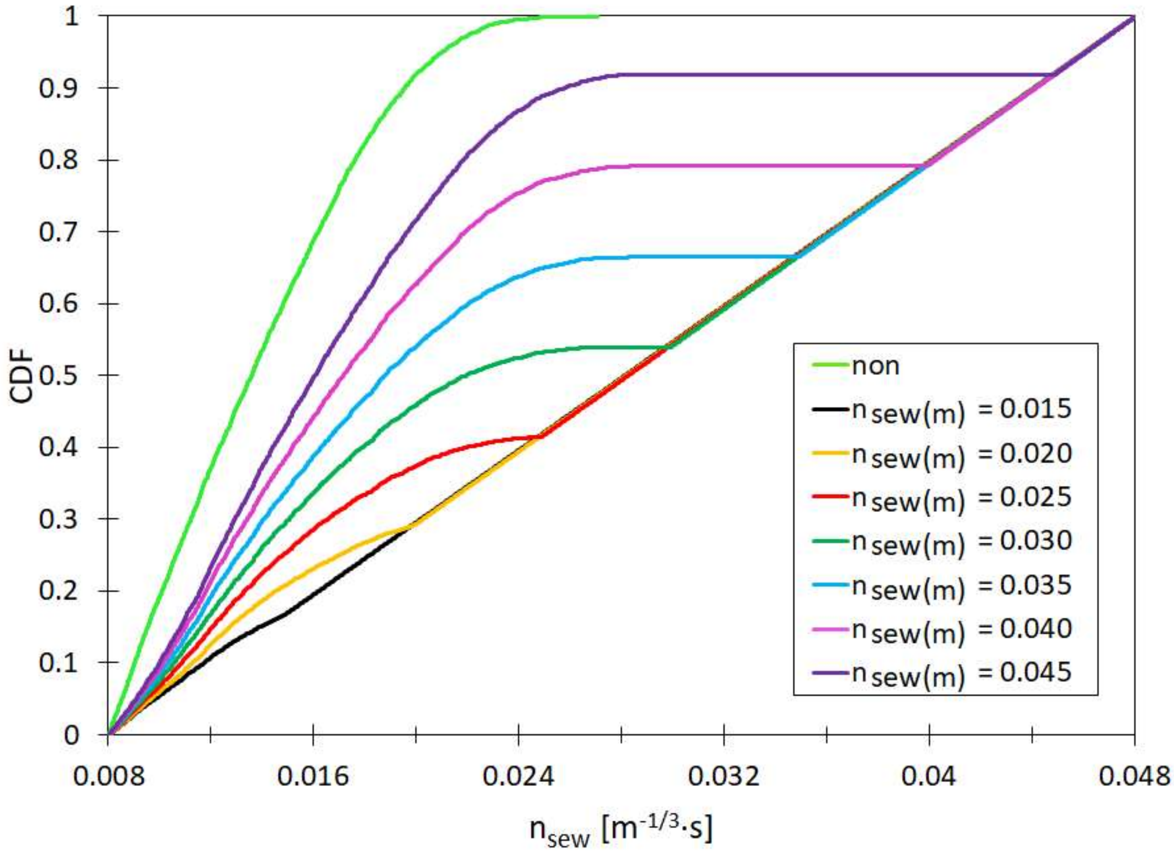

Figure S19. Empirical distributions of Manning roughness coefficients for channels (n_{sew}) for $n_{sew(m)}$=0.015 – 0.045 $m^{-1/3}\cdot s$, Imp = 0.35 and Impd = 0.40.